SAE Aerospace
An SAE International Group

AEROSPACE INFORMATION REPORT

SAE AIR1751 | REV. A

Issued 1981-03
Reaffirmed 1991-02
Stabilized 2012-08

Superseding AIR1751

Prediction Method for Lateral Attenuation of Airplane Noise During Takeoff and Landing

RATIONALE

This document has been determined to contain basic and stable technology which is not dynamic in nature.

STABILIZED NOTICE

This document has been declared "Stabilized" by the SAE A-21 Aircraft Noise Measure and Noise Aviation Emission Modeling Committee and will no longer be subjected to periodic reviews for currency. Users are responsible for verifying references and continued suitability of technical requirements. Newer technology may exist.

TO PLACE A DOCUMENT ORDER: **Tel: 877-606-7323 (inside USA and Canada)**
Tel: +1 724-776-4970 (outside USA)
Fax: 724-776-0790
Email: CustomerService@sae.org
SAE WEB ADDRESS: **http://www.sae.org**

SAE values your input. To provide feedback on this Technical Report, please visit
http://www.sae.org/technical/standards/AIR1751A

1. BACKGROUND: The prediction of noise at points on the ground laterally displaced from the projection of an airplane flight path, e.g., as required for prediction of contours of equal noise levels, requires a knowledge of sound-propagation phenomena. The attenuation of the sound from an airplane in flight depends upon wave divergence (spherical spreading) and atmospheric absorption, in addition to ground, meteorological, and engine/airplane installation effects. The latter three effects give rise to what is referred to herein as lateral attenuation. As the airplane flies at lower altitudes, there is a transition from air-to-ground lateral attenuation to overground lateral attenuation.

   The SAE A-21 Committee on Aircraft Noise undertook in 1979 the development of a uniform and consistent method for the prediction of lateral attenuation. The project was divided into two phases: (1) A short-term phase in which correlations of flight data were made using frequency-weighted and time-integrated measures of the noise, such as Effective Perceived Noise Level (EPNL) and Sound Exposure Level (SEL), see Appendix A; and (2) A long-term phase in which the effects of various sound-propagation phenomena on one-third-octave-band sound pressure levels could be considered. The phenomena would include ground reflection effects, refraction effects, and airplane shielding effects, as well as other ground and engine/airplane installation effects. This Aerospace Information Report is directed to the short-term phase in order to produce an interim prediction method as soon as possible.

2. PHYSICAL ASPECTS OF LATERAL ATTENUATION: Lateral attenuation of airplane noise depends on the elevation angle, and on distance to the side of the flight track. For equal distances, the noise level at a point lateral to an airplane's flight track can be different from the noise level directly below the airplane as a result of attenuation due to ground effects (surface absorption and reflection), meteorological effects such as wind and temperature gradients, and to effects of the airplane installation, such as source shielding.

   The geometrical model assumed in deriving lateral attenuation as considered herein is shown schematically in Figure 1. Point Q on the flight track in the ground plane lies below the linear flight path. Point S on the flight path is located at the nearest distance of approach to point Q ($\overline{QS}$ = d). Point P is displaced normal to the flight track by lateral distance $\overline{QP} = \ell$. The distance between point P and point S is $\overline{PS} = r = \sqrt{\ell^2 + d^2}$, the slant range. The elevation angle β is defined such that $\tan \beta = d/\ell$.

   For purposes of estimating lateral attenuation, consider a situation whereby the airplane is at point S' on an auxiliary flight path parallel to and above the previous flight path, such that $\overline{QS'} = d' = r$, the slant range of the previous case. In both cases, engine power setting, airplane configuration and airspeed are considered to be identical. The difference between the noise level L_Q at point Q when the airplane is flying along the auxiliary flight path and the noise level L_P at point P at the sideline when the airplane is flying along the original flight path is equal to $L_Q - L_P \equiv \Lambda$. The noise level difference Λ, in decibels, is defined as lateral attenuation with respect to point P, i.e., attenuation due to ground effects, meteorological effects, and to installation effects, for an airplane that is airborne.

---

*Editorial Change 6-01-81

In order to develop a prediction method for lateral attenuation, data were collected from all available sources (see Appendix B). These data exhibited variability due to a number of effects. Although spherical spreading and atmospheric absorption effects were assumed to be accounted for by considering the difference in noise levels at the same slant range, other residual effects were present. These residual effects included differences due to ground characteristics, and to meteorological and installation effects. Part of the observed variability in the data correlations was attributed to these residual effects. Additional data variability was attributed to characteristics of the source noise. Noise spectra vary with engine type, installation and power setting. Ground characteristics depend on surface cover, soil type and soil moisture content. With regard to the atmosphere, values and gradients of temperature, humidity, wind speed and direction, and the intensity of atmospheric turbulence play a role in determining sound attenuation. For installation effects, jet shielding is affected by the number of engines and the configuration of engine installations. Airframe shielding due to the presence of such items as the fuselage, nacelles, and flaps in the noise propagation paths may produce significant effects. On some airplane configurations, wing wakes and trailing vortices may interfere with propagation. Data variability from these effects was found to be largest at low elevation angles, where lateral attenuation is also largest (see Appendix B).

Consideration was given as to whether lateral attenuation was a function of lateral, or sideline, distance as well as the elevation angle β. Above some elevation angles and distances, it appeared from the data correlations that lateral distance did not significantly affect the magnitude of the lateral attenuation, but that the elevation angle β was the principal geometrical parameter when the airplane was airborne. However, for the limiting case when the airplane was on the ground, other data showed that the lateral distance had a significant effect on the measured attenuation. Clearly there must be a transition region between the two cases of air-to-ground and overground propagation, in which the lateral attenuation is a function of both elevation angle and lateral distance. (see Appendix C).

Using the available data, and the selected method of analysis, it was not possible to distinguish among the separate effects contributing to lateral attenuation. Therefore, a single "average" curve (Figure 3) of lateral attenuation as a function of airplane elevation angle β was derived, for use with all jet airplanes. The recommended method for predicting lateral attenuation was derived from noise level data for turbojet and turbofan-powered airplanes, and applicability to propeller driven airplanes has not been established. The average curve pertains to long-range air-to-ground attenuation. As discussed in Section 5 below, it may be utilized with the recommended curve (Figure 2) for overground attenuation to give lateral attenuation values in the full range of elevation angle ($0° < \beta < 90°$), as shown in Equation (3) below, the values being functions of both elevation angle and lateral distance.

3. OVERGROUND ATTENUATION: In order to develop a prediction method for overground attenuation, recourse was had to the comprehensive work of Parkin and Scholes, carried out for the Building Research Establishment in the United Kingdom (see References 1 and 2).

As discussed in Appendix C, the Parkin and Scholes results were utilized to derive a single curve of overground attenuation $G(\ell)$ vs. lateral distance ℓ, for the case of airplane elevation angle $\beta = 0°$, as shown in Figure 2. It is estimated that the curve of Figure 2 represents the experimental data of References 1 and 2 and the other data sources described in Appendix C within $\pm$ 3 dB. The curve of Figure 2 gives a constant attenuation of about 14 dB for lateral distances greater than 914 meters (3,000 ft) and may be represented mathematically by the function $G(\ell)$, where ℓ is in meters:

$$G(\ell) = 15.09 \left(1 - e^{-2.74 \times 10^{-3} \ell}\right), \text{ dB}, \quad 0 \leq \ell \leq 914\text{m (3,000 ft)},$$

and

$$G(\ell) = 13.86 \text{ dB}, \quad \ell > 914\text{m (3,000 ft)}$$

It should be noted that the specific value $G(\ell) = 13.86$ for large ℓ was chosen for consistency with the mathematical formulation of Equation (2b) of Section 4.0 below, representing long-range air-to-ground attenuation for $0 \leq \beta \leq 60°$. As discussed in Appendix C, although all the overground data were taken statically and did not include full installation effects, it was necessary, in the absence of further data, to apply the recommended Equation 1 for $G(\ell)$ to EPNL or SEL measures, in order to be compatible with the long-range air-to-ground regime discussed in Section 4.0.

4. LONG-RANGE AIR-TO-GROUND ATTENUATION: Curves of average lateral attenuation were submitted for each of the seventeen data-sets listed in Table B-1 of Appendix B. Data used in deriving the average curves were obtained from tests conducted under atmospheric and general test conditions similar to those required for aircraft noise certification. The resulting recommended prediction curve is shown in Figure 3. The variation in the average lateral attenuation curves from the individual data-sets from which the prediction curve was derived was such that 90 percent of these curves for elevation angles greater than 3° were within ± 2 dB of the prediction curve in Figure 3 (see Appendix B). The recommended prediction curve for $\Lambda(\beta)$ in decibels shown in Figure 3 was fitted by the equation (with β in degrees):

$$\Lambda(\beta) = 3.96 - 0.066\beta + 9.90e^{-0.13\beta}, \text{ dB}, \quad 0° \leq \beta \leq 60°,$$

and

$$\Lambda(\beta) = 0, \text{ dB}, \quad 60° < \beta \leq 90°.$$

The prediction curve in Figure 3 was derived for the time-integrated measures of EPNL and SEL. Consideration was also given to the possible application of Figure 3 to other noise measures such as maximum perceived noise level, or maximum A-weighted sound level. Insufficient information was available to verify the applicability of Figure 3 to these measures, although the available evidence indicated that the curve of Figure 3 might also be applicable to them.

5. LATERAL ATTENUATION IN THE TRANSITION REGION: Because only a relatively small amount of lateral attenuation data had been correlated as a function of both elevation angle and lateral distance, it was not possible to define the dependence of lateral attenuation on elevation angle and lateral distance for cases when the airplane was airborne and lateral distance was relatively small. However, it was recognized that there must be a transition between the long-range air-to-ground attenuation prediction curve (Figure 3) and the overground attenuation prediction curve (Figure 2). As discussed in Appendix C, data of Source 12 of Section 8.0 showed excellent agreement with the long-range air-to-ground prediction curve at long distances, as well as approaching the overground values for small elevation angles. It is recommended that the transition region be represented by a function formed from the product of the functions describing the overground and air-to-ground curves. This function termed $\Lambda(\beta,\ell)$, is given in decibels by:

$$\Lambda(\beta,\ell) = \frac{G(\ell)\,\Lambda(\beta)}{13.86}, \text{ dB}.$$

where $G(\ell)$ and $\Lambda(\beta)$ are given in Equations (1) and (2) respectively. The constant 13.86 is recognized to be the limit of $G(\ell)$ at long range and the limit of $\Lambda(\beta)$ at $\beta = 0°$.

6. SUMMARY OF LATERAL ATTENUATION PREDICTION METHOD:

1. During ground roll, overground attenuation is determined by Equation 1 or the curve shown in Figure 2.

2. For all cases where the aircraft is airborne, lateral attenuation is determined by Equation 3 or by multiplying G from Figure 2 by Λ from Figure 3 and dividing the product by 13.86 (Equation 3). For lateral distances greater than 914 meters (3,000 ft), the long-range attenuation Λ from Figure 3 may be used directly.[1]

7. REFERENCES FOR OVERGROUND ATTENUATION DATA:

1. Parkin, P.H. and Scholes, W.E., The Horizontal Propagation of Sound from a Jet Engine Close to the Ground, at Radlett. J. Sound and Vibration (1964) 1, 1-13.

2. Parkin, P.H. and Scholes, W.E., The Horizontal Propagation of Sound from a Jet Engine Close to the Ground, at Hatfield. J. Sound and Vibration (1965) 2(4), 353-374.

8. SOURCES OF LATERAL ATTENUATION DATA UTILIZED:

1. Anon., Noise Certification Data for A300B, Aerospatiale, unpublished.

2. Anon., Noise Certification Data for Fanjet Falcon G and Falcon 50, AMD/BA[2], unpublished.

3. Anon., Lateral Attenuation of 727 and 747, Boeing, unpublished.

4. Anon., Lateral Attenuation of BAC 1-11 and Concorde, British Aerospace, unpublished.

5. Anon., Noise Certification Data for Learjet 24, Bolt Beranek and Newman, unpublished.

6. Anon., Noise Certification Data for L-1011, Lockheed, unpublished.

7. Anon., DC-9 Flight Demonstrator Program with Refanned JT8D Engines, Final Report, Volume IV, Douglas, NASA CR-134860, July 1975.

8. Anon., DC-10 Sideline Noise Investigations, Douglas, unpublished.

9. Anon., Lateral Attenuation of Military Aircraft Flyover Noise Levels, Air Force Aerospace Medical Research Laboratory, Biodynamics and Bioengineering Division, Wright-Patterson Air Force Base, to be published.

10. DeLapp, R.E., Aircraft Noise Definition, Phase II, Analysis of Flyover Noise Data for DC-8-61 Aircraft, Final Report, Douglas, FAA-EQ-74-5, August 1974.

11. Rickley, E.J., Meteorological Effects Noise Test, Nov. 12, 1977, U.S. Department of Transportation/Transportation Systems Center, unpublished.

12. Willshire, W.L., Jr. and Hilton, D.A., Ground Effects on Aircraft Noise, NASA Technical Memorandum 80185, November 1979.

NOTES: 1. For all cases where the aircraft is airborne, the lateral attenuation is by definition independent of spherical spreading and atmospheric absorption, as discussed in Section 2.0.

2. Avions Marcel Dassault/Breguet Aviation

PREPARED BY
SAE COMMITTEE A-21
AIRCRAFT NOISE

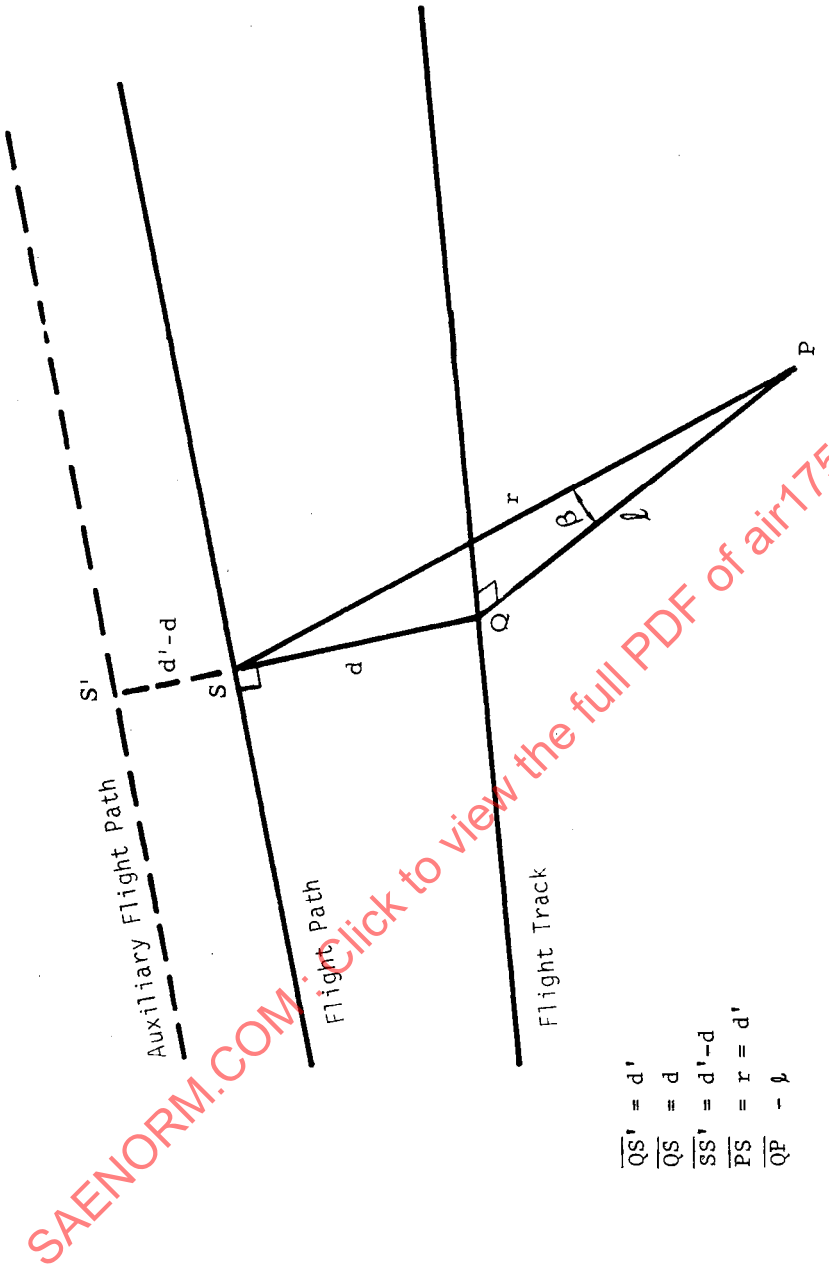

Figure 1. Geometrical model for lateral attenuation.

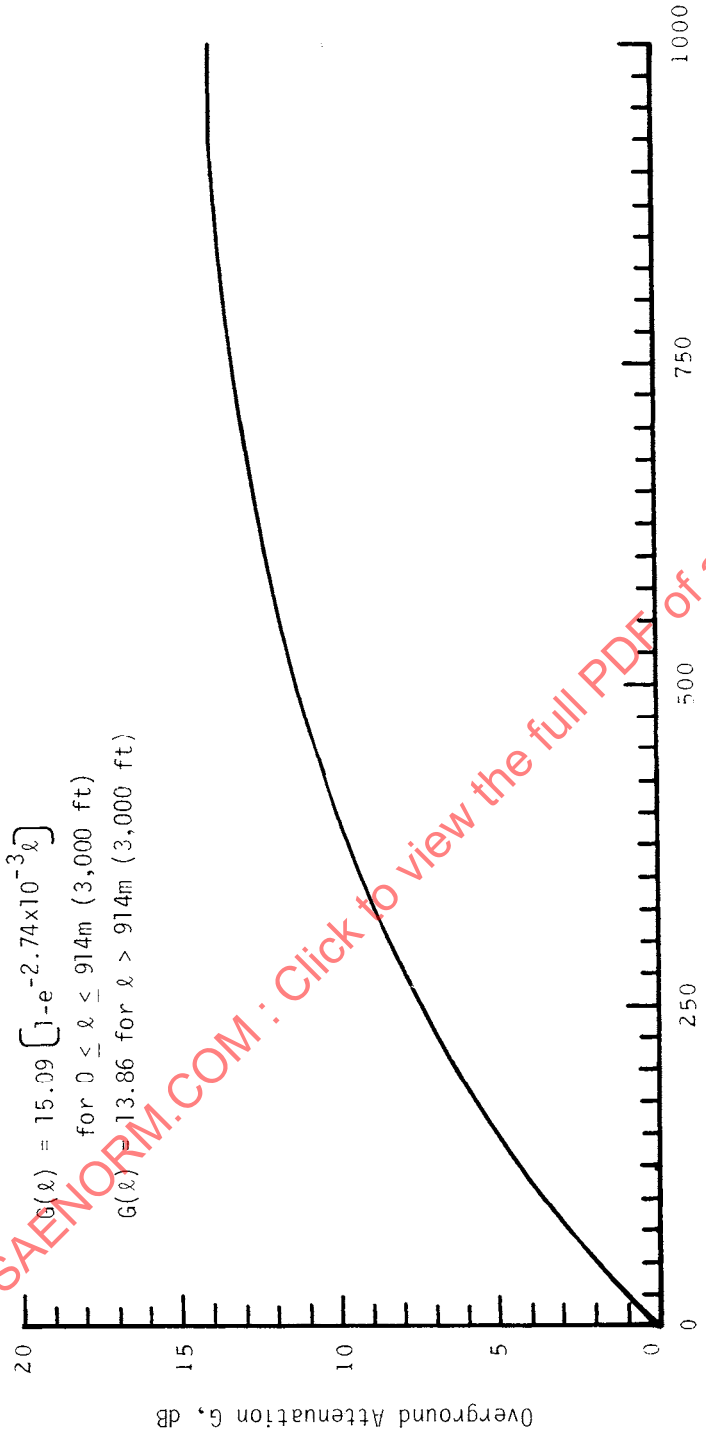

Figure 2. Recommended prediction curve for overground attenuation.

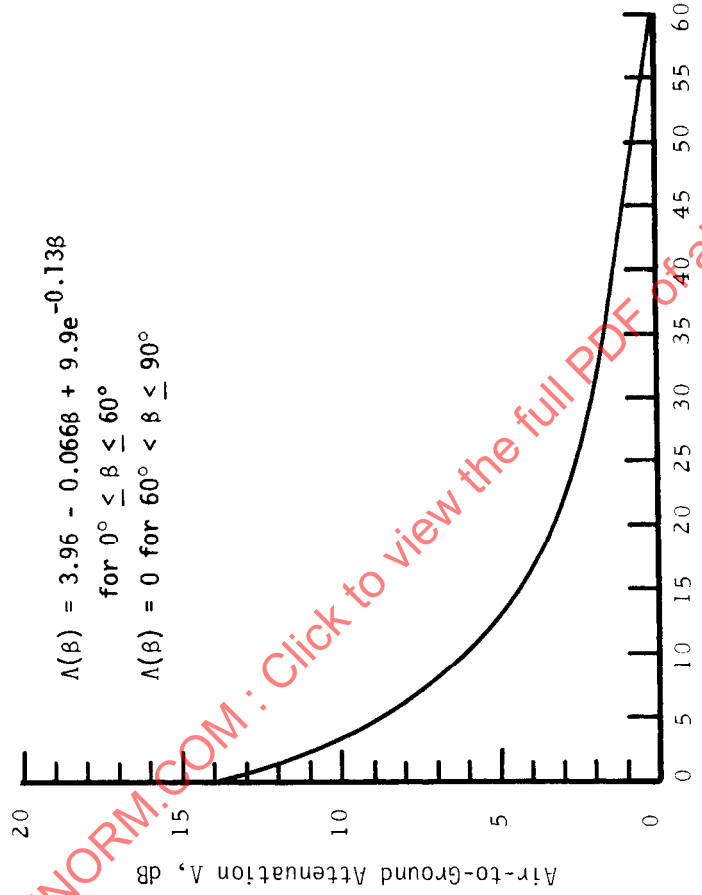

Figure 3. Recommended prediction curve for long-range air-to-ground attenuation.

APPENDIX A

DESCRIPTION OF EFFECTIVE PERCEIVED NOISE LEVEL AND SOUND EXPOSURE LEVEL

GENERAL:

The frequency-weighted and time-integrated noise measures of Effective Perceived Noise Level (EPNL) and Sound Exposure Level (SEL) are defined below in mathematical terms. The measure EPNL is essentially a perceived noise level corrected for time-duration and pure-tone effects. The measure SEL is essentially an A-weighted sound level corrected for time-duration effects.

EFFECTIVE PERCEIVED NOISE LEVEL:

The time-integrated effective perceived noise level is defined, mathematically, as:

$$L_{EPN} = 10 \log_{10} \left[(1/t_E) \int_{t_1}^{t_2} 10^{0.1\, L_{TPN}(t)}\, dt \right]$$

where L_{EPN} is the symbol for effective perceived noise level, t_E is the reference time of 10 seconds for effective perceived noise level, $L_{TPN}(t)$ is the tone-corrected perceived noise level as a function of time t during the duration of a single measurement of aircraft noise, and t_1 and t_2 are the limits of the significant noise time history.

Operationally, Eq. (A1) is implemented by calculating the tone-corrected perceived noise level at discrete intervals of time throughout the duration of the aircraft noise signal. Normally, samples of data are available at 0.5-second intervals and the integral in Eq. (A1) is replaced by a summation as:

$$L_{EPN} = 10 \log_{10} \left[(\Delta t/t_E) \sum_{i=t_1}^{t_2} 10^{0.1\, L_{TPN}(i)} \right]$$

where $\Delta t = 0.5$ seconds, and t_1 and t_2 are usually taken as being the first and last sample times closest to those moments when the tone-corrected perceived noise level is 10 decibels less than the maximum value of the tone-corrected perceived noise level (i.e., the 10-dB-down times).

Equation (A2) can be expressed in terms of the sum of the maximum value of the tone-corrected perceived noise level, L_{TPNM}, and a duration-correction factor, D_E. Thus,

$$L_{EPN} = L_{TPNM} + D_E$$

where

$$D_E = 10 \log_{10} \left[(\Delta t/t_E) \sum_{i=t_1}^{t_2} 10^{0.1\, L_{TPN}(i)} \right] - L_{TPNM}$$

SOUND EXPOSURE LEVEL:

The time-integrated sound exposure level is defined by

$$L_{AE} = 10 \log_{10} \left[(1/t_A) \int_{t_1}^{t_2} 10^{0.1\, L_A(t)} dt \right]$$

where L_{AE} is the symbol for sound exposure level, t_A is the reference time of 1 second for sound exposure level, $L_A(t)$ is the time-varying A-frequency-weighted sound level, and t_1 and t_2 are the so-called "10-dB-down" times before and after the time of occurrence of the maximum value of $L_A(t)$ as defined earlier[1, 2].

As for effective perceived noise level, the time-varying A-weighted sound level is usually available at fixed intervals of time, normally 0.5-seconds long. Thus, Eq. (A5) is replaced by the operational equation

$$L_{AE} = 10 \log_{10} \left[(\Delta t / t_A) \sum_{i=t_1}^{t_2} 10^{0.1\, L_A(i)} \right]$$

where again $\Delta t = 0.5$ seconds and t_1 and t_2 are taken to be the 10-dB-down times from the maximum A-weighted sound level, L_{AM}.[3]

In parallel to the formulation of Eq. (A3), Eq. (A6) can also be expressed in terms of the maximum A-weighted sound level and a duration factor as

$$L_{AE} = L_{AM} + D_A$$

where the duration factor, D_A, for sound exposure level is defined as

$$D_A = 10 \log_{10} \left[(\Delta t / t_A) \sum_{i=t_1}^{t_2} 10^{0.1\, L_A(i)} \right] - L_{AM}$$

NOTES:

1. In International Standard IS 3891, Acoustics--Procedure for Describing Aircraft Noise Heard on the Ground, sound exposure level is known by the symbol L_{AX} instead of L_{AE}.

2. Sound exposure level is sometimes referred to as noise exposure level in some Federal documents.

3. A specialized version of sound exposure level called single-event noise exposure level, SENEL, has been used in the California Airport Noise Standard. In SENEL, sound level is integrated over the duration during which it exceeds a specifiable threshold sound level. When the maximum sound level exceeds the threshold sound level by 10 decibels, SENEL is identical to SEL. When the maximum level exceeds the threshold sound level by 20 decibels or more, SENEL is approximately 0.3dB greater than the sound exposure level as defined above.

APPENDIX B

DEVELOPMENT OF RECOMMENDED METHOD FOR PREDICTION OF LONG-RANGE AIR-TO-GROUND LATERAL ATTENUATION

The prediction curve for long-range air-to-ground lateral attenuation A in decibels (shown in Figure 3 of the AIR text) was chosen as representative of the "average" for all turbojet and turbofan powered airplanes. This curve was derived from data of seventeen test series on various airplanes, in the form of curves of average lateral attenuation as a function of elevation angle β. The seventeen airplane data sets contained a total of 1,702 measurements. Test heights ranged from a low of 10m (33 ft) to a maximum of 2,743m (9,000 ft). Lateral distances extended from essentially zero to a maximum of 2,743m (9,000 ft). Specific details on the data sets for individual airplanes are available from the data sources noted in Table B-2. Although there were differences among the seventeen data-sets as regards test procedures, number of test points, and data evaluation procedures, similar "weighting" was given to each data-set in developing the prediction curve. The variation in the resultant average lateral attenuation curves was such that it was estimated that 90 percent of the curves for elevation angles greater than 3° were within ± 2 dB of the prediction curve of Figure 3.

Thus, for elevation angles greater than about 10°, all of the curves were within the ± 2 dB spread, while in the elevation angle range between 3° and about 10° (where the data scatter is largest), only four of the seventeen curves were outside of the ± 2 dB spread (see Figure B-2). For the application of the lateral attenuation prediction curve of Figure 3, the curve was fitted by the mathematical equation shown on the figure, which for calculation purposes may be utilized for all elevation angles down to 0° in the prediction of attenuation in the transition region between overground attenuation and long-range air-to-ground attenuation.

The average lateral attenuation curves from the seventeen data-sets are shown in Figure B-1, where two groups are shown in order to improve visualization of the differences among curves. The upper group shows the curves for commercial transport airplanes, while the lower group shows the curves for business jet and military airplanes. In Figure B-2 all of the curves of Figure B-1 are compared with the prediction curve of Figure 3 of the AIR. The numerical designations of the data-set curves are keyed to Table B-1, which identifies airplanes, engines, noise measures, and sources of data. Table B-2 lists the sources of the data. Other data-sets examined, not shown in Figures B-1 and B-2, but lying within the range of values shown in Figure B-2, included additional data on some of the airplanes considered. The additional data were given in the noise measures listed in Table B-1, as well as in other noise measures.

As discussed in the AIR text the observed variability in the data correlations is due to a number of effects. Thus, effects of ground characteristics, meteorological conditions, noise source frequency content, engine installation configuration, jet shielding, airframe shielding, and wing-wake and trailing vortex interference were believed to be contributors to the data variability. Examination of the average lateral attenuation curves of Figures B-1 and B-2 gives some insight into the contributions of these effects to the data variability.

The variability in the individual data sets provides an indication of the confidence one might place in the "average" curve recommended in Figure 3 as an interim curve for use with all airplane types. The long-term program of SAE Committee A-21 should yield more definitive information regarding possible curves for individual airplane types which are more appropriate than a single "average" curve. It is recognized that the variability in attenuation shown in Figures B-1 and B-2 could result in significant effects on predicted noise contour areas. Thus, if during the interim period, a user determines that lateral attenuation estimates obtained using the "average" curve for any specific airplane type or types are too high or too low, he may wish to consider some adjustments to the "average" curve for his specific application. In cases where adjustments are used, the fact should be noted on any results so obtained in order to avoid errors in interpretation.

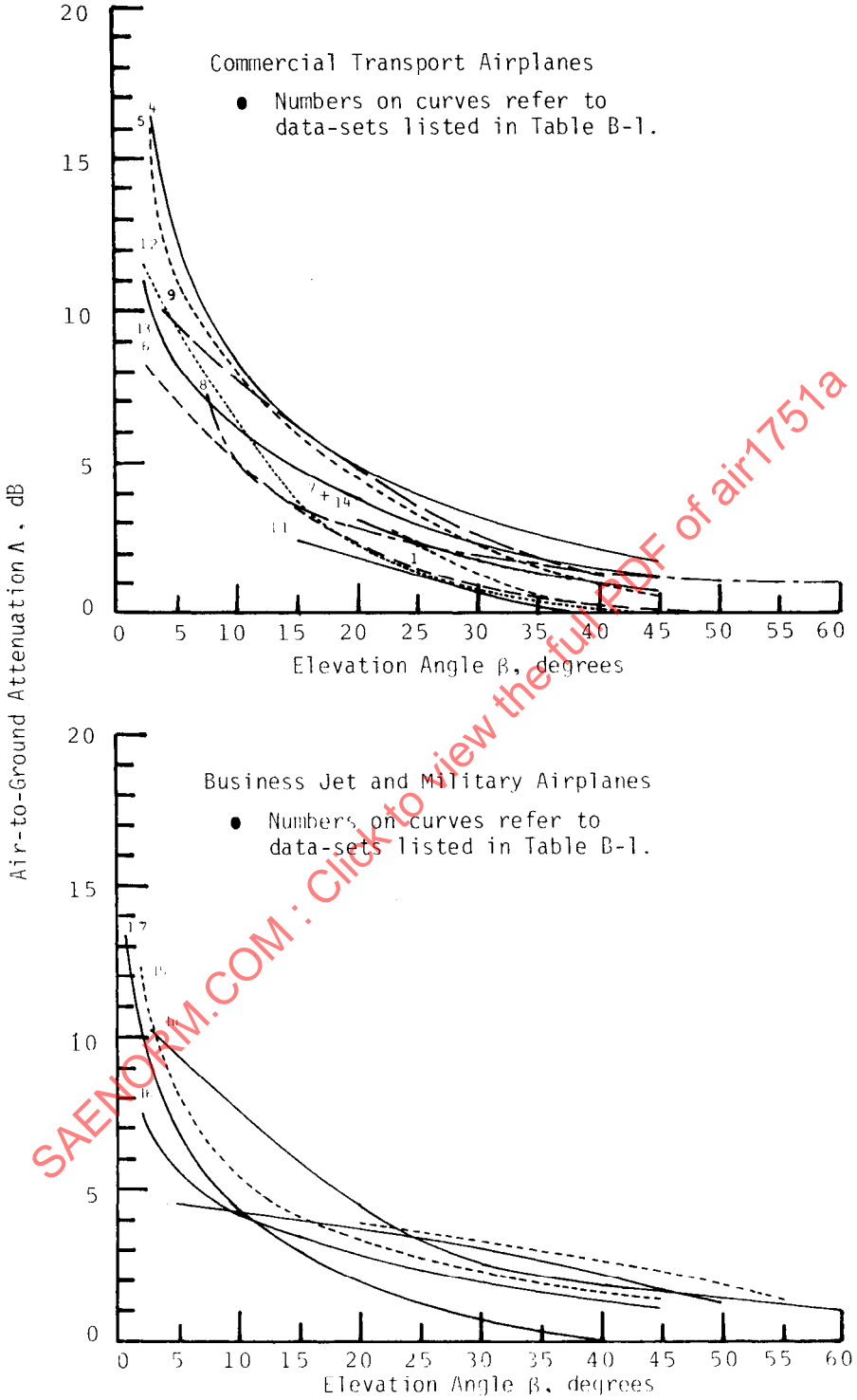

Figure B-1. Average lateral attenuation curves used to develop long-range air-to-ground attenuation prediction curve.

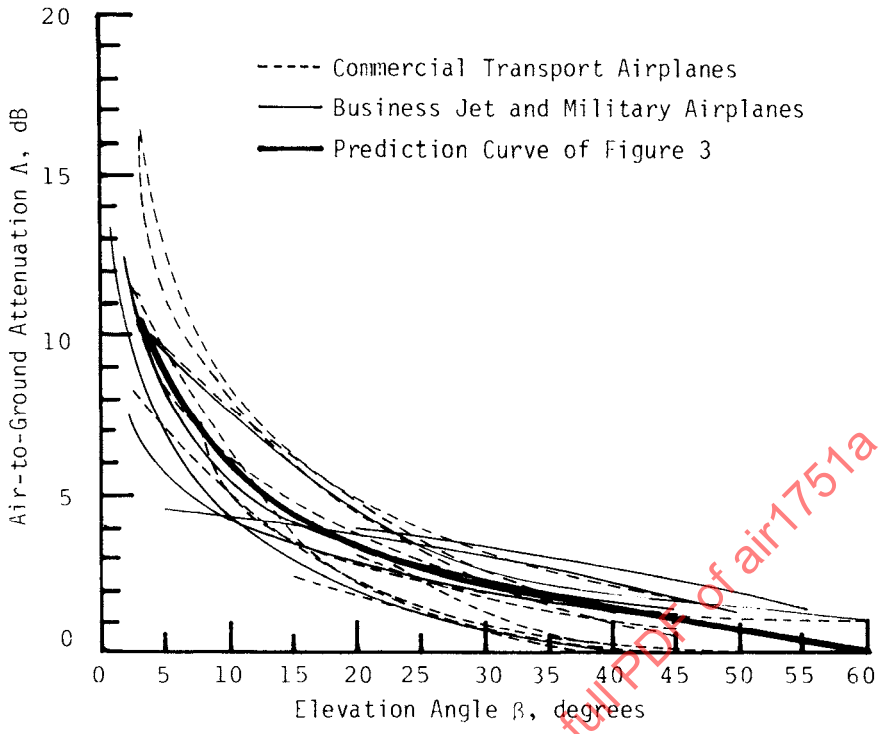

Figure B-2. Prediction curve for long-range air-to-ground attenuation compared with average lateral attenuation curves of Figure B-1.

TABLE B-1

DATA-SETS FOR LONG-RANGE AIR-TO-GROUND ATTENUATION

	AIRPLANE	ENGINES	NOISE MEASURE	SOURCES OF DATA (3)
1.(1)	AIRBUS INDUSTRIE A300B-4	2 x CF6-50C2 & 2 x JT9D-59	EPNL	1
2.	AMD/BA(2) FANJET FALCON G	2 x ATF 3-6	EPNL	2
3.	AMD/BA(2) FALCON 50	3 x TFE 731-3	EPNL	2
4.	BOEING 727-100	3 x JT8D-9	EPNL	3
5.	BOEING 727-100	3 x JT8D-9 + ejector suppressors	SEL	3
6.	BOEING 727-100 (DOT Test)	3 x JT8D-7	SEL	11
7.	BOEING 747SR	4 x JT9D-7	EPNL	3
8.	BRITISH AEROSPACE BAC-1-11-200	2 x Spey 506	PNL	4
9.	CONCORDE 001 (Prototype) and 102 (Pre-Production)	4 x Olympus 593-3B & 4 x Olympus 593-602	EPNL or PNLM	4
10.	GATES LEARJET 24	2 x CJ610-6	SEL or ALM	5
11.	LOCKHEED L-1011-1 and L-1011-200	3 x RB.211-22B & 3 x RB.211-524B	EPNL	6
12.	MCDONNELL-DOUGLAS DC-8-61	4 x JT3D-3B	EPNL	10
13.	MCDONNELL-DOUGLAS DC-9-30 Refan	2 x JT8D-109	EPNL or ALM	7
14.	MCDONNELL-DOUGLAS DC-10-10 and DC-10-30 and DC-10-40	3 x CF6-6D 3 x CF6-50A/C & 3 x CF6-50C1 3 x JT9D-59A & 3 x JT9D-20	EPNL	8
15.	MCDONNELL-DOUGLAS F-15	2 x F100-PW-100	SEL	9
16.	MCDONNELL-DOUGLAS F-18	2 x F404-GE-400	SEL	9
17.	NORTHROP T38A (far engine idle)	2 x J85-5	EPNL	12

NOTES:

(1) Numbers refer to curve legend on Figure B-1.

(2) Avions Marcel Dassault/Breguet Aviation.

(3) See Table B-2 for sources of data.

TABLE B-2

SOURCES OF LATERAL ATTENUATION DATA UTILIZED

1. Anon., Noise Certification Data for A300B, Aerospatiale, unpublished.

2. Anon., Noise Certification Data for Fanjet Falcon G and Falcon 50, AMD/BA[1], unpublished.

3. Anon., Lateral Attenuation of 727 and 747, Boeing, unpublished.

4. Anon., Lateral Attenuation of BAC 1-11 and Concorde, British Aerospace, unpublished.

5. Anon., Noise Certification Data for Learjet 24, Bolt Beranek and Newman, unpublished.

6. Anon., Noise Certification Data for L-1011, Lockheed, unpublished.

7. Anon., DC-9 Flight Demonstrator Program with Refanned JT8D Engines, Final Report, Volume IV, Douglas, NASA CR-134860, July 1975.

8. Anon., DC-10 Sideline Noise Investigations, Douglas, unpublished.

9. Anon., Lateral Attenuation of Military Aircraft Flyover Noise Levels, Air Force Aerospace Medical Research Laboratory, Biodynamics and Bioengineering Division, Wright-Patterson Air Force Base, to be published.

10. DeLapp, R.E., Aircraft Noise Definition, Phase II, Analysis of Flyover Noise Data for DC-8-61 Aircraft, Final Report, Douglas, FAA-EQ-74-5, August 1974.

11. Rickley, E.J., Meteorological Effects Noise Test, November 12, 1977, U.S. Department of Transportation/Transportation Systems Center, unpublished.

12. Willshire, W.L., Jr. and Hilton, D.A., Ground Effects on Aircraft Noise, NASA Technical Memorandum 80185, November 1979.

NOTE:
1. Avions Marcel Dassault/Breguet Aviation

APPENDIX C

DEVELOPMENT OF RECOMMENDED METHODS FOR PREDICTION OF LATERAL ATTENUATION FOR OVERGROUND AND TRANSITION REGIONS

OVERGROUND ATTENUATION:

Some of the most extensive research into overground noise attenuation was carried out by Parkin and Scholes at the Building Research Establishment at the airports at Radlett and Hatfield in the United Kingdom, (Refs. 1 and 2). This work was not only carried out over a reasonably large range of distances, but also throughout the year from summer to winter months. It was found that there was quite a seasonal variation of attenuation, and the lowest attenuation was found during the winter months. Although some of the Hatfield data resulted in rather low lateral attenuation levels, the authors of References 1 and 2 have concluded that the data generally agree to within about 2 dB, due mainly to attenuation frequency shift. The "winter days" data from Radlett were used in the derivation of the overground attenuation prediction method given herein, so that the results are expected to be conservative, i.e., the predicted attenuation values should be lower than those that are likely to be encountered in practice. In this connection it must be appreciated, that because of the large refraction effects that can be caused by wind and temperature gradients, the attenuation of sound over long distances close to the ground is subject to wide variations around the predicted values. Predictions made by the method proposed herein provide an indication of the average attenuation which might be experienced under moderate temperature and humidity conditions when the atmosphere was calm and rather homogeneous.

The data reported by Parkin and Scholes indicated large variations of overground attenuation with frequency. This result implied that any measure of overground attenuation will be dependent on spectral content. An attempt was therefore made to assess the variation of ground attenuation with distance for a number of different engines to see how large the total effect of the spectral variation might be. For this purpose the spectra at takeoff thrust for the engines listed in Table C-1, varying in bypass ratio from 0 to 6, were used with the attenuation spectrum provided by Parkin and Scholes to estimate spectral changes for distances of up to 1,250m (4,101 ft) from the source. The spectra calculated at various distances were then combined to determine the overground attenuation. Figure C-1 shows the result of this computation for takeoff thrust settings. The analysis was then repeated for the approach case, the results of which are shown in Figure C-2.

Examination of the results in Figures C-1 and C-2 showed the rather remarkable result that the curves for all these different engines were within a band that was about ± 2.5 dB wide for the takeoff case, and ± 2 dB wide for the approach case. These variations were consistent with the variability of the curves used to develop the long-range air-to-ground attenuation curve of Figure 3 of the AIR text. It was also noted that the overground attenuation stabilized to a constant value at around 914m (3,000 ft) sideline distance.

For the take-off case, a mean (arithmetic average) curve was derived. A similar curve was derived for the approach case. The two average curves are shown in Figure C-3, and are within 1 dB of each other. In view of the variability in the data from which they were derived, it appeared that the results for both takeoff and approach cases could be adequately represented by a single curve, shown as the recommended overground attenuation prediction curve in Figure C-4. This curve gives a constant attenuation of 13.86 dB for sideline distances greater than 914 meters (3,000 ft). It may be represented mathematically by the function $G(\ell)$, where ℓ is in meters:

$$G(\ell) = 15.09 \left[1 - e^{-2.74 \times 10^{-3} \ell}\right] \text{ dB}, \quad 0 \leq \ell \leq 914\text{m (3,000 ft)}$$

and

$$G(\ell) = 13.86 \text{ dB}, \quad \ell > 914\text{m (3,000 ft)}$$

The specific value $G(\ell) = 13.86$ for large ℓ was chosen for consistency with the mathematical formulation of Equation (2a) of Section 4.0 above, representing long-range air-to-ground attenuation for $0 \leq \beta \leq 60°$.

TRANSITION REGION:

The development discussed in the previous section of this appendix furnishes a method for prediction of overground lateral attenuation for cases when the airplane is on the ground (elevation angle $\beta = 0°$). The recommended prediction equations for such cases (Equations C-1 above and Equations 1 of the AIR text) give overground lateral attenuation as a function only of lateral distance. The development discussed in Appendix B furnishes a companion method for prediction of long-range air-to-ground lateral attenuation for cases when the airplane is airborne (elevation angle $\beta > 0°$). The recommended prediction equations for such cases (Equations 2 of the AIR text) give long-range air-to-ground lateral attenuation as a function only of elevation angle. However, there clearly must be a transition region between the two cases of overground and air-to-ground propagation, in which the lateral attenuation is a function of both lateral distance and elevation angle.

In order to formulate a method for prediction of lateral attenuation in the transition region, it was noted that available experimental results were essentially limited to the data from the T-38A tests of Source 12 in Section 8.0 of the AIR text, where data were correlated for four lateral distances. However, these data showed excellent agreement with the long-range air-to-ground formulation at large lateral distances, and approached the overground formulation for small elevation angles (see Figure C-5). Accordingly, it is recommended that lateral attenuation in the transition region be approximated by a function formed from the product of the overground and air-to-ground functions, mathematically described by:

$$\Lambda(\beta,\ell) = \frac{G(\ell)\ \Lambda(\beta)}{13.86},\ \text{dB}$$

where $G(\ell)$ and $\Lambda(\beta)$ are given in Equations 1 and 2 of the AIR text respectively. The constant 13.86 is recognized to be the limit of $G(\ell)$ at large lateral distance and of $\Lambda(\beta)$ at $\beta = 0°$. Figure C-5 shows comparisons of the T-38A measured lateral attenuation data with predictions (Equation C-2) for lateral distances of 190m (623 ft), 370m (1,213 ft), 765m (2,510 ft), and 1330m (4,364 ft). The predictions were within 1 to 2 dB of the measured values for the two shorter distance results, and within approximately 0.5 dB for the two longer distance results. The agreement between measurements and predictions was of the same order, or better, as the variability noted for the data used to develop the overground or the long-range air-to-ground lateral attenuation prediction methods.

NOISE MEASURES:

A difficulty is encountered when consideration is given to the quantity used to measure lateral attenuation in the overground and transition regions. All overground attenuation data was for engines operating under static conditions, and clearly a duration correction in this context is not appropriate. Hence, the curves derived for overground attenuation were not in terms of time-integrated measures such as Effective Perceived Noise Level (EPNL) or Sound Exposure Level (SEL). However, there was a fair amount of evidence that the decay with distance of Maximum Perceived Noise Level (PNLM) is similar to the decay of EPNL or SEL. In most cases, the decay of maximum A-weighted sound level (ALM) was within 1 dB of the decay of the time-integrated measures. Therefore, it was concluded that the prediction methods for the overground and transition regions could be applied to maximum as well as time-integrated quantities. This is, in fact, a pessimistic assumption in terms of the time-weighted measures, since overground attenuation will reduce the forward and aft-radiated noise produced by an airplane accelerating or decelerating along a runway more than it reduces the maximum value. Thus, the duration term decreases more rapidly with lateral distance than the maximum noise level.

INSTALLATION EFFECTS:

In the above consideration of overground attenuation and the transition to long-range air-to-ground attenuation, no attempt was made to allow for the effect of jet or airframe shielding. There is very limited reliable evidence on the effect of shielding in this situation. Likewise, in the case of the derivation of the long-range air-to-ground attenuation formulation, it was felt that there was insufficient evidence to separate the effects of shielding from the total lateral attenuation, so the final long-range air-to-ground lateral attenuation curve derived was a mean curve which included the effects of both excess ground attenuation and an average shielding effect.

As mentioned above, the scatter in overground lateral attenuation introduced by the variability in atmospheric conditions is very large, and a view could be taken that the effects of shielding are small compared with these effects. Taking this view, it would not be unreasonable to ignore the effects of shielding until more evidence becomes available and a more adequate allowance can be made. It is proposed that this approach should be adopted for the shorter-term solution of this AIR, but that the effects of shielding should be more fully investigated and allowed for in any longer-term studies.

REFERENCES:

1. Parkin, P.H. and Scholes, W.E., The Horizontal Propagation of Sound from a Jet Engine Close to the Ground, at Radlett. J. Sound and Vibration (1964) 1, 1-13.

2. Parkin, P.H. and Scholes, W.E., The Horizontal Propagation of Sound from a Jet Engine Close to the Ground, at Hatfield, J. Sound and Vibration (1965) 2(4), 353-374.

TABLE C-1

ENGINE TYPES USED IN OVERGROUND ATTENUATION STUDY

Manufacturer	Type	Bypass Ratio (Takeoff Thrust)	Takeoff Thrust Rating, Sea Level, Static, kN (lb)
(1)			
1. P & W A	JT8D-109	2 : 1	73.8 (16,600)
2. Rolls Royce	Viper 632 a) conical nozzle b) ejector nozzle c) 8-lobe nozzle	0	17.8 (4,000)
3. Rolls Royce	Spey Mk 512-14 DW	0.6 : 1	55.8 (12,550)
4. R-R/SNECMA	Olympus 593	0	167.7 (37,700)
5. R-R/SNECMA	M45H-01	3 : 1	35.0 (7,865)
6. Rolls Royce	RB.211-22B	5 : 1	186.8 (42,000)
7. C.F.M. International	CFM56	5.9 : 1	97.9 (22,000)
8. Avco Lycoming	ALF 502A	6 : 1	27.6 (6,200)

NOTES:

(1) Numbers refer to curve legends on Figures C-1 and C-2.